Electrical properties and transport mechanisms in Ge-Sb-Te thin films

P. LAZARENKO[a], A. SHERCHENKOV[a], S. KOZYUKHIN[b,c], A. BABICH[a], S. TIMOSHENKOV[a], A. SHULIATYEV[a], V. KUDOYAROVA[d]
[a]*National Research University of Electronic Technology, Bld. 1, Shokin Square, Zelenograd, Moscow, 124498, Russia*
[b]*Kurnakov Institute of General and Inorganic Chemistry, RAS, Leninsky Pr., 31, Moscow, 119991, Russia*
[c]*Department of Chemistry, National Research Tomsk State University, Tomsk, 634050, Russia*
[d]*Ioffe Physico-Technical Institute, RAS, Politekhnicheskaya, 26, St-Petersburg, 194021, Russia*

Influence of the composition variation along the quasi-binary line GeTe-Sb_2Te_3 on the transport mechanisms of thin films was investigated. Three regions with different current-voltage dependencies were established. Composition dependence of the energy diagrams was analyzed. Position of the trap levels controlling transport mechanisms, and density of traps were estimated. Obtained results showed that electrical properties of thin films can be sufficiently varied with moving along the quasi-binary line, which is important for the optimization of PCM technology.

(Received November 2, 2015; accepted February 10, 2016)

Keywords: Phase change memory, Ge-Sb-Te, Electrical properties, Transport mechanisms

1. Introduction

Non-volatile memory devices are actively developed now, which is stimulated by the drawbacks of the most widespread flash technology [1]. Promising alternative non-volatile memory types at this moment are considered to be magnetoresistive (MRAM), ferroelectric (FRAM), resistive (RRAM) and phase change (PCM) memories [1-4]. The later is one of the main candidates for new generation of memory devices, which claim to become universal, joining advantages of non-volatility and high rate dynamic memory with increased radiation resistance.

Principle of the operation of PCM is based on the sufficient difference in the optical and/or electrical properties of the active material in amorphous and crystalline states, which can be initiated by the low-energy external influences. This determined appearance of two main types of PCM memory devices - optical and electrical PCM.

However, despite of the progress in PCM technology and commercial success of optical discs, electrical PCM is not widespread till now due to the number of problems, and necessity to improve technology. One of the problems is connected with the need of decreasing the data processing time.

Currently, the most promising materials for the PCM application are considered to be chalcogenide materials on the basis of ternary system Ge-Sb-Te (GST). Most widely investigated and used as a programmable material for PCM is $Ge_2Sb_2Te_5$ on the quasi-binary line GeTe-Sb_2Te_3 due to the complex of properties [5-8]. However, improving the data processing time needs modification of the PCM material in order to alter thermal properties and increase crystallization rate.

Three compounds exist on this quasi-binary line (Fig. 1): $Ge_2Sb_2Te_5$ (GST225), $GeSb_2Te_4$ (GST124), and $GeSb_4Te_7$ (GST147), which corresponds to the ratio $(GeTe)_n(Sb_2Te_3)_m$ (n : m = 2 : 1; 1 : 1; 1 : 2), respectively.

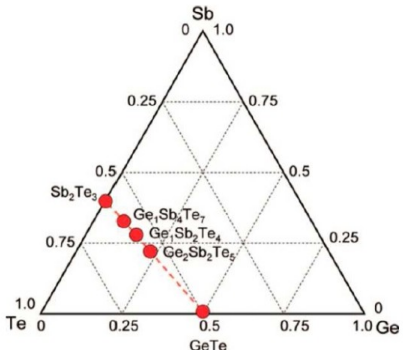

Fig. 1. Quasi-binary line GeTe-Sb_2Te_3 with three compounds: $Ge_2Sb_2Te_5$, $GeSb_2Te_4$, and $GeSb_4Te_7$

N. Yamada and coauthors showed [5] that thermal properties of GST materials sufficiently depend on the position on the quasi-binary line GeTe-Sb_2Te_3, and crystallization rate increases with moving along this line from GeTe to Sb_2Te_3. But many questions related to the electrical properties, in particular transport mechanisms, and their correlation with composition and position on the quasi-binary line are still open. The study of the transport mechanisms is necessary for controlling the physical properties of programmable materials, and development of effective methods for improving and optimization of phase change memory technology. Therefore, the aim of this work

is to examine the influence of the composition variation along the quasi-binary line $GeTe\text{-}Sb_2Te_3$ on the electrical properties of thin films, including transport mechanisms and energy parameters.

2. Experimental

The alloys GST225, GST124, and GST147 were synthesized in evacuated ($2\ 10^{-5}$ Pa, ILMVAC CDK-180, Germany) and sealed fused quartz ampoules (6 mm in diameter) by conventional melt-quenching technique in a rocking furnace as was described elsewhere [9]. Thin films were prepared by thermal evaporation of the synthesized materials in vacuum. Substrate temperature during the deposition did not exceed 50°C.

According to the X-ray diffraction (Rigaku D/MAX, Cu Kα λ=0.15481 nm) synthesized materials were polycrystalline and had a trigonal phase, while as-deposited films were amorphous. Annealing of thin films at temperatures higher than 150 °C is accompanied by the crystallization of the films.

Elemental analysis of thin films was investigated by Rutherford backscattering spectroscopy (RBS, E_d = 1.0, E_α = 2.7 MeV, φ = 135 °). Overlapping of the peaks due to the neighbor position of Sb and Te in the Periodic table allowed to determine only ratios Ge/(Sb + Te), which were close to the theoretical values for all studied compounds (Table 1).

Table 1. Results of RBS measurements

Composition	Ge/(Sb+Te)	
	Experiment	Calculation
GST147	1/(10.7 ± 0.4)	1/11
GST124	1/(6.1 ± 0.2)	1/6
GST225	1/(3.4 ± 0.1)	1/3.5

The spectroscopic ellipsometry measurements were carried out using a variable angle ellipsometer (ELLIPSE-1881A) in the wavelength range of 380-1050 nm with a step of 10 nm at an incident angle of 70°.

For the measurements of the electro-physical properties and current-voltage characteristics planar structures containing Al electrodes with fixed interelectrode distances, and deposited upon them GST thin films were fabricated on oxidized c-Si substrates.

For investigation of electro-physical characteristics specialized manually controlled measuring set-up was used.

Set-up includes following functional blocks: measuring cell with resistive heater; temperature measuring system on the basis of calibrated thermocouple (type K), power source (AKIP-1114) and multimeter (Keithey 2002); measurement system of electro-physical properties includes a voltage control unit (NI6008) and picoammeter (Keithley 6485). Measurements of current-voltage characteristics (CVC) were carried out in the isothermal regime at the temperature range from room temperature to 70 °C with the steps of 10 °C and voltage range from 0.1 to 10 V with step of 0.1 V.

3. Results and discussion

Measurements of CVCs (Fig. 2) of the amorphous thin films of different compositions in the range from 293 to 355 K showed the existence of tree voltage ranges with different I-V dependencies for weak ($E < 10^3$ V/cm, $U < 0.7$ V), middle (10^3 V/cm $< E < 10^4$ V/cm, 0.7 V $< U <$ 7 V) and high ($E > 10^4$ V/cm, $U >$ 7 V) electric fields indicating on the different mechanisms of charge carrier transport.

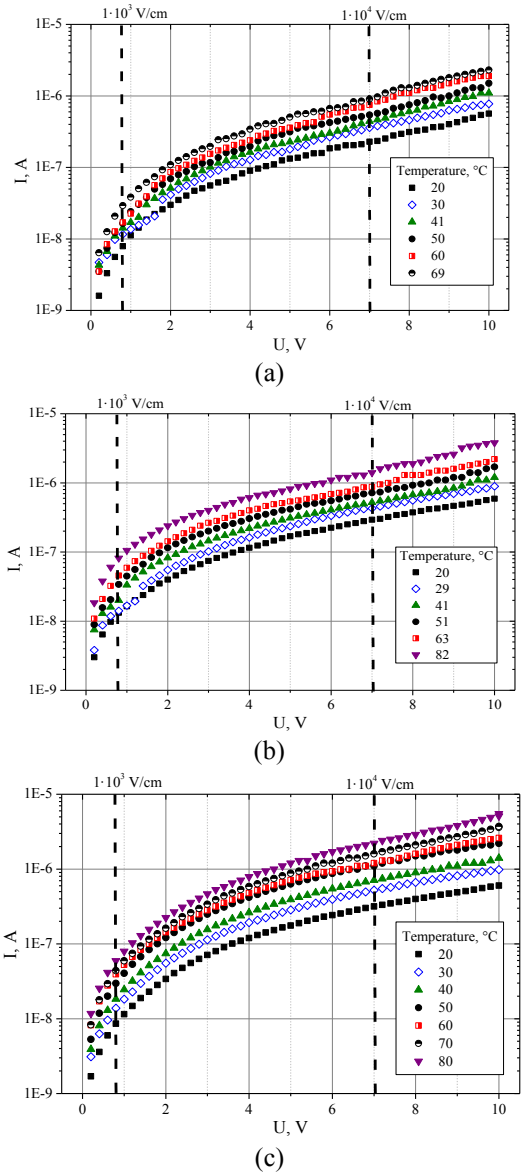

Fig. 2. Current-voltage characteristics for the amorphous films: (a) GST147, (b) GST124, (c) GST225

Ohmic regions at low electric field intensity ($E < 10^3$ V/cm) were observed for all studied compounds. The results of temperature dependences of conductivity are shown in the Fig. 3.

As can be seen from the figure, exponential temperature dependences of conductivity were observed for all amorphous thin films, which indicate on the activation character of the conductivity, and are characteristic for chalcogenide glassy semiconductors [10]. In this case, temperature dependence of the conductivity is described by the following expression:

$$\sigma = \sigma_0 \exp\left(-\frac{E_a}{kT}\right), \quad (1)$$

where σ is the conductivity, σ_0 is a constant, E_a is the activation energy of conductivity, k is the Boltzmann constant, and T is the absolute temperature.

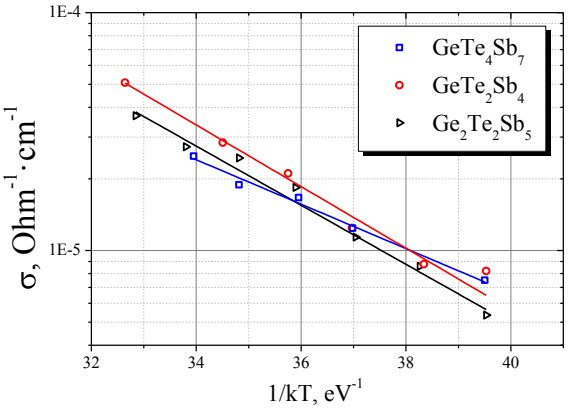

Fig. 3. Temperature dependences of conductivity for GST147, GST124, and GST225 thin films.

Activation energies of conductivity were calculated for all films and are presented in the Table 2. Energy band gap (E_g) and Urbach energy (E_0) for investigated compounds were obtained by spectrophotometry, and also presented in the table.

Table 2. Energy parameters for GST147, GST124, and GST225 thin films.

Composition	E_g (opt.), eV	E_a, eV	E_0, eV
$GeSb_4Te_7$	0.50	0.22	0.09
$GeSb_2Te_4$	0.54	0.28	0.08
$Ge_2Sb_2Te_5$	0.61	0.29	0.13

With using of the Mott - Davis (MD) model of the energy bands [11], and taking into account experimental results, the energy band diagrams for amorphous GST thin films were proposed (Fig. 4). We also took into consideration results of thermoelectric power measurements for studied thin films, which indicated on the dominating p-type conductivity of GST films.

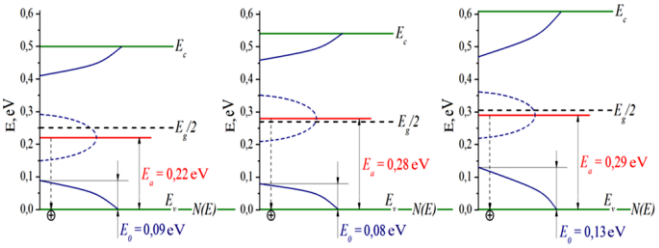

Fig. 4. Energy diagrams for Ge-Sb-Te thin films: a – GST147; b - GST124; c - GST225

As can be seen from the figure, values of the activation energies for conductivity of amorphous thin films are close to the middle of the mobility gap, except for GST124. For this composition activation energy is slightly higher $E_g/2$. Conductivity activation energy increases with moving in the direction from GST147 to GST225 on the quasi-binary line, which can be due to the variation of the optical gap width and density of states in it.

Urbach parameter characterizes width of the band tails in the mobility gap. Obtained values of E_0 (see Table 2) for thin films of GST124 (0.08 eV) and GST147 (0.09 eV) are close and less than for GST225 (E_0 = 0.13 eV), which indicates that thin films of GST124 and GST147 have less disordered structure in comparison with GST225.

We used two-channel model proposed by P.Nagels [12] for modeling of the dependences of σ versus 1/T. According to this model transport of charge carriers by the delocalized states of the valence band and localized states of the valence band tail can simultaneously contribute to the p-type conductivity of the chalcogenide glassy semiconductors. So, the sum of two exponents characterizing the charge carrier transport by these states was used for the description of the conductivity

$$\sigma = \sigma_{0} \exp\left(-\frac{E_F - E_V}{kT}\right) + \sigma_{0h} \exp[-(E_F - E_0 + W)/kT], \quad (2)$$

where the first term corresponds to the transport of the charge carriers by the delocalized states, and second – to the hopping transport by the localized states of the valence band tail (σ_0' and σ_{0h} are pre-exponential factors), W is the energy required for hopping.

Fig. 5 present results of the simulation of the temperature dependences of the conductivities for investigated thin films. As can be seen from the figure results of simulation and experimental data are close enough. It should be noted, however, that such simulation does not allow strictly determine parameters σ_0, σ_{0h} and W, therefore possible ranges of these parameters can be estimated, which are shown in Table 3.

CVCs in the middle electric field intensity range ($10^3 < E < 10^4$ V/cm) has power dependences for all investigated compounds. Fig. 6 presents CVCs for the GST225 thin film in double logarithmic scale at the middle electric field strength range.

Power dependence of CVCs is typical for space charge limited current (SCLC) and is described by an equation:

$$j = KV^m \quad (3)$$

where K is coefficient depending on film thickness, trap density distribution and conductivity of investigated materials.

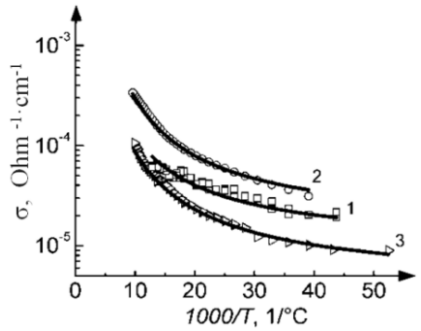

Fig. 5. Dependences of the conductivities on 1000/T: 1 - GST147; 2 - GST124; 3 - GST225. Markers denote the experimental data, solid lines – results of simulation

Table 3. Energy parameters for thin films on the basis of compounds on the quasi-binary line Sb_2Te_3 – GeTe

Compound	Parameters		
	σ_0, Ohm^{-1}·cm^{-1}	σ_{0h}, Ohm^{-1}·cm^{-1}	W, eV
GST147	0.08÷0.12	0.0008÷0.0012	0.005÷0.015
GST124	0.45÷0.60	0.0045÷0.0060	0.005÷0.015
GST225	2.0÷3.0	0.01÷0.02	0.005÷0.015

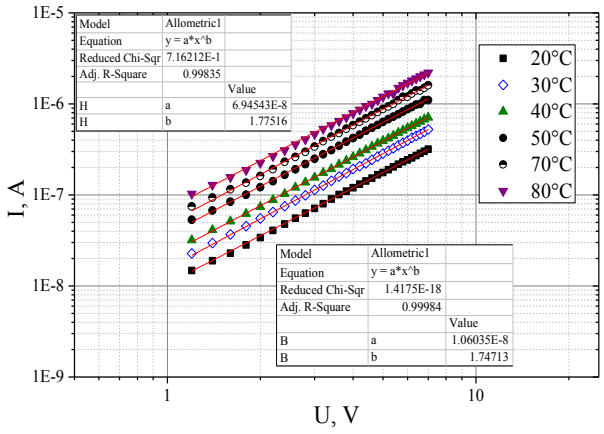

Fig. 6. Current-voltage characteristics for the GST225 thin film in double logarithmic scale at the middle electric field strength range

Application of an electric field to the dielectric is accompanied by the appearance of current due to the electrons injected from the cathode according to the theory [13]. It should be noted that these electrons create space charge in the material. Following equation is typical for SCLC in ideal dielectric [13]

$$j \approx \varepsilon_0 \varepsilon \mu \frac{V^2}{L^3} \quad (4)$$

where ε_0 is dielectric constant, ε is permittivity, μ is charge carrier mobility, L is thickness of the dielectric.

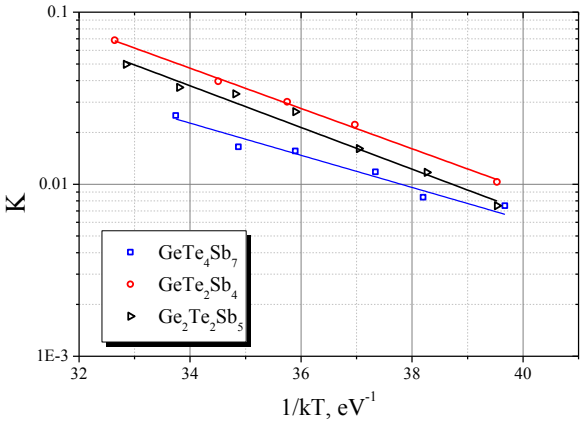

Fig. 7. Temperature dependences of coefficient K for GST147, GST124, and GST225 thin films.

Second order current-voltage dependences corresponding to the ideal SCLC were also observed in semiconductors when charge carriers are transferred by band states, and when they are captured on the discrete levels of localized states [14].

However analysis of CVC for the studied thin films has shown that for all compounds the power m (Eq. 3) deviates from the value of two. Rose theory [14] declares that the presence of traps in the band gap can significantly influence injected current. M. Lampert [15] has shown that the position of the traps and their distribution can cause deviation of the power m from the value of two. Similar deviations from the second order dependence were observed experimentally in [16, 17], in which disordered semiconductors including the chalcogenide glassy semiconductors were investigated.

Furthermore, exponential dependences of the coefficient K on 1/kT were established for all samples (Figure 7). According to [13] nonlinearity of I-V characteristics in p-type semiconductors associated with the capture of injected charge carriers on the discrete localized levels can be described by the following expression:

$$j \approx \theta \varepsilon_0 \varepsilon \mu \frac{V^2}{L^3}, \quad (5)$$

where θ is factor characterizing the ratio of free charge carriers to carriers captured on the traps.

So,

$$\theta = \frac{p}{p_t} \approx \frac{N_V g_i}{N_t} \exp\left(\frac{E_V - E_t}{kT}\right), \quad (6)$$

where p and p_t are concentrations of free carriers and carriers captured on the traps, respectively, N_V is the effective

density of states in valence band, N_t is the density of states at the E_t level, E_V is top energy of the valence band, E_t is the trap level controlling transport mechanism, g_i is a degree of degeneration, which is taken equal to ½, and kT is the thermal energy.

Thus, the coefficient K in the Eq. 3 can be expressed as:

$$K = K_0 \exp\left(-\frac{E_t - E_V}{kT}\right), \quad (7)$$

where

$$K_0 = \varepsilon\mu \frac{N_V g_t}{N_t L^3}. \quad (8)$$

Assuming that the mobility has a weak activation character, and using Eq. 7, positions of level E_t restricting the current transport, and values of pre-exponential factor K_0 for the investigated thin films can be estimated. In addition, with using of Eq. 8 and assuming that $\varepsilon \approx 16$ [17], $\mu \approx 20$ cm^2/V·c [18], $N_v \approx 10^{19}$ cm^{-3} [13], $g_i = ½$ the density of states N_t can be estimated. Results of these estimations are presented in the Table 4.

Table 4. Parameters characterizing SCLC for GST147, GST124, and GST225 thin films.

Compound	E_t, eV	N_t, cm^{-3}
GST147	0,20	$2\cdot10^{16}$
GST124	0,27	$9\cdot10^{14}$
GST225	0,28	$8\cdot10^{14}$

In the case of low applied voltage the holes injecting from aluminum contact are captured by deep traps, but CVC is linear until the average concentration of the injected charge carriers becomes comparable with the concentration of thermally generated carriers. With increasing concentration of the injected free holes in the valence band the position of quasi-Fermi level begins to shift closer to the valence band. As a result the position of the level E_t determining activation energy in the middle electric field intensity range is somewhat closer to the top of the valence band than that for the low electric field strength intensity (E_a).

With moving along the quasi-binary line GeTe-Sb_2Te_3 position of this level shifts (Fig. 8), which can be due to the decrease of the band gap and redistribution of the density of states.

Estimation showed that with the transition from GST225 to GST147 density of states N_t increases from $8\cdot10^{14}$ to $2\cdot10^{16}$ cm^{-3}, which correlates with the variation of the band gap width. This is explained by the increase of the concentration of weaker chemical bonds Sb-Te compared with stronger chemical bonds Ge-Te.

Nonlinear dependences at high electric field intensity ($E > 10^4$ V/cm) were observed for all compounds. Overview of the experimental electrophysical data for GST thin films is presented in the work [19], and comparative analysis of different dc transport mechanisms was carried out. In this work M. Nardone has shown that Poole-Frenkel ionization, space-charge limited current, field-induced delocalization of tail states are possible candidates for explanation of nonlinear I-V characteristics for high electric field strength range in GST thin films. However, further investigations are needed to clarify transport mechanism in this range.

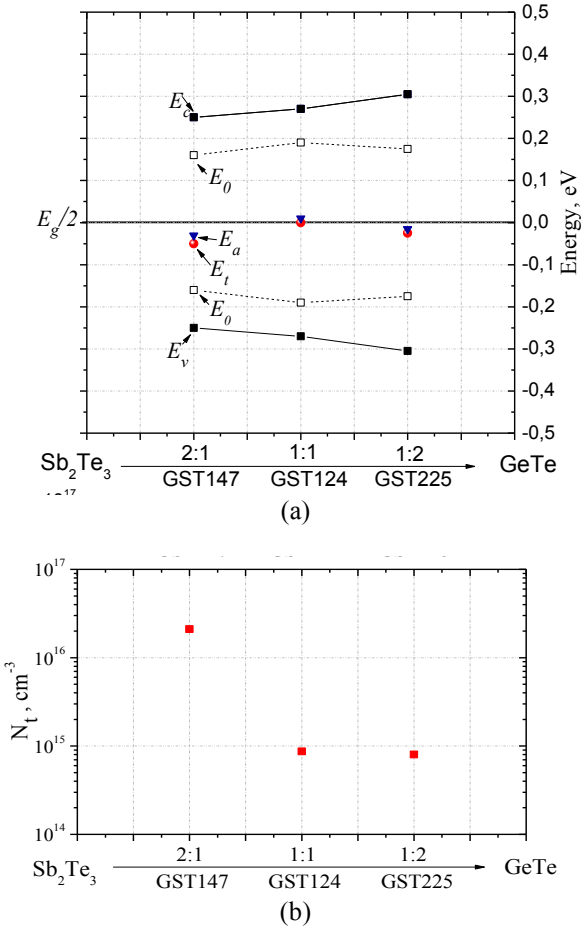

Fig. 8. Composition dependence of the SCLC parameters for GST147, GST124, and GST225 thin films: a – energy band diagram; b – density of states.

4. Conclusions

Influence of the composition variation along the quasi-binary line GeTe-Sb_2Te_3 on the transport mechanisms in thin films was investigated. Three regions with different current-voltage dependencies were established. Composition dependence of the energy diagrams was analyzed. Position of the trap levels controlling transport mechanisms, and density of traps were estimated. Obtained results showed that electrical properties of thin films can be sufficiently varied with moving along the quasi-binary line, which is important for the optimization of PCM technology.

Acknowledgements

This work was supported by the Ministry of Education and Science of Russian Federation (project ID: RFMEFI57514X0096).

References

[1] M. H. Krynder, C. S. Kim, IEEE Transactions on Magnetics **45**, 3406 (2009).
[2] A. N. Belov, O. V. Pyatilova, M. I. Vorobiev, Advances in Nanoparticles **3**, 1 (2014).
[3] A. V. Solnyshkin, I. L. Kislova, M. V. Silibin, D. A. Kiselev, Ferroelectrics **469**, 144 (2014).
[4] J. J. Yang, D. B. Strukov, D. R. Stewart,Nature Nanotechnology **8**, 13 (2013).
[5] N. Yamada, E. Ohno, K. Nishiuchi, N. Akahira, M. Takao. J. Appl. Phys. **69**, 2849 (1991).
[6] G. W. Burr, M. J. Breitwisch, M. Franceschini, D. Garetto, K. Gopalakrishnan, B. Jackson, B. Kurdi, C. Lam, L.A. Lastras, A. Padilla, B. Rajendran, S. Raoux, R.S. Shenoy, J. Vac. Sci. Technol. B **28**, 223 (2010).
[7] H.-S. P. Wong, S. Raoux, S.B. Kim, J. Liang, J. P. Reifenberg, B. Rajendran, M. Asheghi, K. E. Goodson, Proceedings of the IEEE **98**, 2201 (2012).
[8] S. Raoux, W. Wełnic, D. Ielmini. Chem. Rev. **110**, 240 (2010).
[9] S. A. Kozyukhin, A. A. Sherchenkov, E. V. Gorschkova, V. Kh. Kudoyarova, A. I. Vargunin, Phys. Status Solidi C **7**, 848 (2010).
[10] N. Mott, Electrons in disordered structures, Mir, Moscow (1967).
[11] N. F. Mott, E. A. Davis, Electron Processes in Non-Crystalline Materials, Clarendon Press, Oxford (1979).
[12] M. H. Brodsky, Topics in Applied Physics, **36**, Springer-Verlag Berlin, Heidelberg, New York (1979).
[13] M. A. Lampert, P. Mark. Current Injections in Solids, Academic Press, New York (1970)
[14] A. Rose, Phys. Rev, **97**(6), 1538 (1955).
[15] L. F. Marsal, J. Pallare`s, X. Correig, J. Appl. Phys. **79**(11), 8493 (1996).
[16] R. L. Weisfield, J. Appl. Phys **54**, 6401 (1983).
[17] E. Prokhorov, J. J. Gervacio-Arciniega, G. Luna-Bárcenas, Y. Kovalenko, F.J. Espinoza-Beltran, G. Trapaga, J. Appl. Phys. **113**, 113705 (2013).
[18] J. M. Yáñez-Limón, J. González-Hernández, J. J. Alvarado-Gil, I. Delgadillo, H. Vargas, Phys.Rev. B. **52**(23), 16321 (1995).
[19] M. Nardone, M. Simon, I.V. Karpov, V.G. Karpov, J. Appl. Phys. **112**, 071101 (2012).

*Corresponding author: sergkoz@igic.ras.ru